Chinese Chemical Letters 37 (2026) 112049

Contents lists available at ScienceDirect

Chinese Chemical Letters

journal homepage: www.elsevier.com/locate/cclet

# Metal-organic framework materials for encapsulation, release and delivery of essential oils: Engineering strategies and challenges

Junfeng Huang[a,b], Hongxin Chen[b], Yan Liao[b], Xiaowen Zhang[b], Zengzhu Zhang[c], Xiaoyu Su[b], Zihong Xie[b], Biao Li[b], Baode Shen[a,b], Pengfei Yue[a,b,*]

[a] State Key Laboratory for the Modernization of Classical and Famous Prescriptions of Chinese Medicine, Jiangxi University of Chinese Medicine, Nanchang 330004, China
[b] Key Laboratory of Modern Preparation of Traditional Chinese Medicine, Ministry of Education, Jiangxi University of Chinese Medicine, Nanchang 330004, China
[c] Department of Pharmaceutics, 908th Hospital of Joint Logistics Support Force of PLA, Nanchang 330000, China

ARTICLE INFO

*Article history:*
Received 12 June 2025
Revised 29 October 2025
Accepted 31 October 2025
Available online 1 November 2025

*Keywords:*
Essential oils
Metal-organic framework materials
Encapsulation
Release
Delivery
Engineering strategies

ABSTRACT

Essential oils (EOs) are widely present in aromatic plants and possess a wide range of significant pharmacological activities such as antibacterial, antioxidant and anti-tumor properties. They have broad application prospects in medical care, food, agriculture and other fields. However, their poor stability poses substantial challenges that significantly hinder their development and practical application. Metal-organic framework materials (MOFs), characterized by highly controllable structures, large specific surface areas, and stimuli-responsive release properties, have been extensively utilized in various fields such as drug delivery and food preservation. Due to their capacity to encapsulate and deliver EOs, MOFs have garnered considerable attention. In this review, we systematically summarize the structural features, types, and characteristics of MOFs, as well as the recent advancements in their application for controlled EO release. Furthermore, we focus on discussing engineering strategies aimed at enhancing the encapsulation, release, and delivery of EOs using MOFs. Finally, we briefly outline the existing challenges in the delivery of EOs using MOFs and present well-reasoned insights into prospective directions for future research.

© 2025 Published by Elsevier B.V. on behalf of Chinese Chemical Society and Institute of Materia Medica, Chinese Academy of Medical Sciences.

## 1. Introduction

Essential oils (EOs) are a unique class of aromatic volatile substances with medicinal value extracted from fragrant plants. They are mainly composed of terpene compounds, alcohols, phenols, aldehydes, ketones and esters [1]. EOs not only exhibit aromatic properties but also demonstrate a wide range of pharmacological activities, including antibacterial [2], anti-inflammatory [3], antioxidant [4], and anti-tumor [5] effects. Although EOs possess numerous advantages, their poor stability remains the critical issue that restricts their practical application. EOs are inherently volatile and susceptible to oxidation [6,7].

Metal-organic framework materials (MOFs), as a subclass of coordination polymers, are porous crystalline materials formed by metal ions/clusters and organic ligands through coordination bonds [8]. The core advantages of MOFs in delivering EOs are as follows: (1) The high porosity and confinement effect enable efficient encapsulation of the volatile components in EOs, thereby significantly reducing volatilization and oxidation losses [9,10]. (2) Pore engineering design, integrated with stimulus-responsive mechanisms, enables intelligent regulation of EOs release and achieves multimodal delivery [11,12]. (3) Surface functional group modification can enhance the comprehensive performance of MOFs, such as targeting ability, stability and antibacterial activity [13–15]. However, although previous studies have extensively examined the individual properties and conventional applications of EOs and MOFs [16–18], recent advances have started to focus on MOF-based EO encapsulation systems [19–21]. While several reviews have summarized their applications in agriculture and food science [22], a comprehensive theoretical framework remains lacking—particularly with regard to the rational design, functionalization strategies, and interdisciplinary integration of these composite materials in broader application contexts. Crucially, in MOF-mediated EO delivery systems, key knowledge gaps remain regarding the structural engineering principles required to optimize delivery efficiency and achieve multifunctional performance.

Therefore, this review provides a systematic analysis of the structural characteristics, classifications, and physicochemical prop-

* Corresponding author.
*E-mail address:* pengfeiyue@jxutcm.edu.cn (P. Yue).

https://doi.org/10.1016/j.cclet.2025.112049
1001-8417/© 2025 Published by Elsevier B.V. on behalf of Chinese Chemical Society and Institute of Materia Medica, Chinese Academy of Medical Sciences.

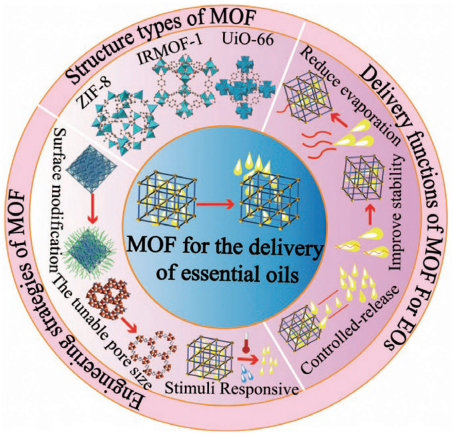



**Fig. 1.** Schematic diagram of the structure types of MOF, the delivery functions of MOF for EOs, and the engineering strategies of MOF for delivering EOs.

erties of MOFs, while summarizing recent progress in their application for the encapsulation, controlled release, and targeted delivery of EOs. In contrast to previous studies, this work emphasizes engineering approaches designed to enhance the efficiency of EOs delivery through MOF-based systems, offering innovative perspectives and methodological insights for achieving precise and effective delivery (Fig. 1). Moreover, this study directly addresses key challenges in MOF-based EOs delivery, including intelligent structural design, scalability, and biocompatibility, and provides targeted recommendations for future research, potentially guiding the development of new strategies and practical applications in this emerging field.

## 2. Framework types of MOFs employed in EOs encapsulation and delivery applications

MOFs are a class of porous crystalline materials formed by the self-assembly of metal nodes and multi-dentate organic ligands through coordination bonds. This section will concentrate on presenting the primary types of MOF materials, including representative examples such as zeolitic imidazolate frameworks (ZIFs) with zeolite-like structures, the MIL series developed by the French Institute of Materials, the UiO series from the University of Oslo and cyclodextrin-based MOFs (CD-MOFs). Additionally, their applications in the encapsulation and delivery of EOs will also be discussed. Table S1 (Supporting information) presents the main types of MOFs.

### 2.1. ZIFs

ZIFs are the most representative type of MOFs. Their structure is similar to that of natural zeolites, composed of tetrahedral metal ions (such as $Zn^{2+}$, $Co^{2+}$) coordinated with the nitrogen atoms at the 1,3 positions of imidazole ligands [23]. The bond angle of metal ion-imidazole-metal ion in ZIFs (145°) is consistent with that of Si-O-Si in zeolites, endowing them with the dual advantages of high stability of zeolites and the modifiability of MOFs [24]. Taking ZIF-8 as an example, it was first reported by the Yaghi team. Its crystal structure is formed by the self-assembly of $Zn^{2+}$ and 2-methylimidazole through coordination bonds, presenting rhombohedral or cubic crystal forms. This material has a pore diameter of approximately 11.6 Å, a specific surface area of up to 1947 $m^2/g$, and a pore volume of 0.663 $cm^3/g$. It features high porosity, excellent thermal stability, and pH-responsive properties [25].

Benefiting from its high specific surface area and pH-responsive release characteristics, ZIF-8 demonstrates excellent EO loading capacity and controllable release performance. Ding *et al.* [26] reported that CT@ZIF-8 achieved a loading efficiency of 15.22 % for citral (CT). The material demonstrated good biocompatibility and showed no cytotoxicity against RTG-2 and RTH-149 cell lines when the concentration of released zinc ions was below 12.5 μg/mL [27]. Huang *et al.* [28] developed a core–shell carrier, Magnolol@ZnO–ZIF-8, which released 93.17 % of magnolol within 24 h at pH 5, compared to only 55.66 % at pH 8, highlighting its pronounced pH-dependent release behavior. Through functional modification or composition with other materials, the application potential of ZIF-8 can be further expanded. In the field of food preservation, Min's team constructed a pectin-based "gatekeeper" film with pH/enzyme dual-responsive properties, which enabled the intelligent release of thymol (Thy) (over 86 % release under acidic or enzymatic conditions), extending the shelf life of mangoes and raspberries by 5–7 days [29]. Yang *et al.* [30] constructed a cinnamaldehyde–ZIF-8 system that effectively mitigated water and chlorophyll loss in spinach during storage ($P < 0.05$). In the medical field, Nezhad-Mokhtari *et al.* [20] successfully co-loaded ZIF-8 and chamomile EO by electrospinning to prepare multifunctional nanofiber composites. The resulting material exhibited significant broad-spectrum antibacterial activity, with inhibition zone diameters of 32.3 and 31.2 mm against *S. aureus* and *Escherichia coli*, respectively, and also promoted the proliferation of fibroblasts, demonstrating its dual-function potential for smart wound dressings with combined healing and anti-infection properties. In summary, ZIF-8, as an EO carrier, demonstrates broad prospects for functional customization and practical applications through rational composite engineering design.

### 2.2. MILs

The MIL family is an important subclass of MOFs, typically formed by trivalent metal ions (such as $Cr^{3+}$, $Fe^{3+}$, $Al^{3+}$) and organic ligands (such as terephthalic acid) through self-assembly into highly ordered porous crystal structures. Their typical structures include mesoporous cage-like structures, such as MIL-101(Cr), which has a mesoporous rigid structure with pore diameters ranging from 2.0 nm to 3.4 nm and a specific surface area as high as 5900 $m^2/g$ [31]. In addition, some MIL family materials (such as MIL-53 and MIL-47) exhibit reversible pore size change capabilities. Under external stimuli, these materials can switch between large-pore and narrow-pore forms, thereby achieving dynamic regulation [32,33].

MIL-100(Fe) is a cubic lattice metal-organic framework material constructed by $Fe^{3+}$ metal clusters and benzene-1,3,5-tricarboxylic acid ligands through coordination bonds. Its mesoporous cages contain two pore diameters (25 and 29 Å), which are connected through microporous windows (5.5 and 8.6 Å). The BET specific surface area reaches 1456–2000 $m^2/g$, and the pore volume is 1.25 $cm^3/g$ [34]. Owing to its distinctive porous structural features, MIL-100(Fe) has shown significant advantages in EO delivery and antibacterial applications. Caamano *et al.* [35] prepared mesoporous material MIL-100(Fe) loaded with Thy, with a Thy loading capacity of up to 42 %. After Thy was encapsulated in MIL-100(Fe), its antibacterial performance was significantly enhanced. Experimental results showed that free Thy could reduce the colony-forming units of *Salmonella enteritidis* by 0.40, while Thy-loaded MIL-100(Fe) could reduce the colony-forming units by 1.57, indicating that its antibacterial effect was 93 % higher than that of free Thy. Besides, Pak *et al.* [36] combined MIL-100(Fe) loaded with tea tree EO with κ-carrageenan to form a film, which has excellent ultraviolet blocking properties, appropriate water vapor permeability and broad-spectrum antibacterial properties.

### 2.3. UiOs

The UiOs of MOFs developed by the University of Oslo uses the zirconium oxo cluster $[Zr_6O_4(OH)_4]$ as the metal node and terephthalic acid or its derivatives as organic ligands to construct a three-dimensional porous framework structure with high chemical stability. Cavka *et al*. [37] first systematically reported the synthesis strategy of UiO-66 and its exceptional performance in high-pressure $CO_2$ adsorption. Its strong Zr-O bond and unique octahedral coordination geometry endowed the material with resistance to water, acids and high temperatures. Based on this structural advantage, Kandiah *et al*. [38] first demonstrated that the functionalized UiO-66 could still maintain high thermal stability and chemical stability. Further research by Wu *et al*. [39] revealed that neutron diffraction was used to uncover the controllable "missing linker" defects in UiO-66 (regulated by acetic acid modulator and synthesis time), achieving structural control that increased the pore volume from 0.44 $cm^3/g$ to 1.0 $cm^3/g$ and the specific surface area from 1000 $m^2/g$ to 1600 $m^2/g$. In addition to defect engineering, the morphology and pore size of UiO-66 can also be precisely controlled through other synthetic strategies. Wang *et al*. [40] successfully constructed UiO-66 with controllable particle size (40–200 nm) and hierarchical porous structure (coexistence of micropores and mesopores) by using a co-regulation strategy of dodecanoic acid (DA) and triethylamine (TEA). The Abazari team further clarified the adjustable pore size feature of zirconium-based MOFs. By using the ligand extension strategy, the terephthalic acid ligands in UiO-66 were replaced with biphenyl dicarboxylic acid, resulting in UiO-67, whose pore size expanded from 10.2 Å in UiO-66 to 14.4 Å [41].

The aforementioned studies have established a theoretical foundation for the application of UiO series materials in the field of EO delivery. In the biomedical domain, Zheng *et al*. [42] leveraged the high porosity of UiO-66 to achieve efficient loading of Thy and carvacrol (Car), with loading rates of 79.60 % ± 0.71 % and 79.65 % ± 0.76 %, respectively. *In vitro* release experiments demonstrated that within 72 h, the release rates of Thy and Car reached 77.82 % ± 0.87 % and 76.51 % ± 0.58 %, respectively. In terms of antibacterial performance, the minimum bactericidal concentrations (MBC) of Car@UiO-66 and Thy@UiO-66 against *Candida albicans*, *E. coli*, and *S. aureus* were 0.313, 0.313, and 1.25 mg/mL, respectively. Cytotoxicity tests indicated that even at a concentration of 1.25 mg/mL, both composites maintained cell viability above 50 %. Animal experiments further revealed that the materials effectively promoted the repair of bone defects by modulating the expression of inflammatory factors such as tumor necrosis factor-$\alpha$ (TNF-$\alpha$), interleukin-6 (IL-6), and IL-10, demonstrating good biocompatibility and bone regeneration potential. UiO-based materials also show broad application prospects in the food sector. Zuniega *et al*. [43] encapsulated Thy using carboxyl-functionalized UiO-66-$(COOH)_2$, achieving a loading rate of 46 %. After storage at 25 °C for six days, the composite material maintained an inhibition rate of over 90 % against the spore germination of *Colletotrichum musae*, significantly overcoming the volatility limitation of EOs and extending the duration of antimicrobial activity.

### 2.4. CD-MOFs

CD-MOFs represent a class of porous polymers that result from the self-assembly process where metal ions and CD molecules are linked by coordination interactions. CD-MOFs generally possess high porosity and large specific surface areas, with their internal cavities exhibiting hydrophobic properties, which constitutes one of their key characteristics. The interior of these cavities is densely populated with C–H groups, offering non-polar interaction sites for various molecules. Meanwhile, their outer surfaces are rich in highly polar hydroxyl groups, forming a synergistic effect with the hydrophobic cavities, thereby enabling efficient encapsulation of lipophilic substances and significantly enhancing their solubility in water [44].

Represented by CD-MOF-1, this material has demonstrated remarkable performance in the field of EO delivery. In the area of fruit and vegetable preservation, Yu *et al*. [45] loaded 4-terpineol into $\gamma$-CD-MOF, achieving an encapsulation efficiency of 53.61 % and a loading capacity of 9.31 %. This system significantly delayed the release of 4-terpineol and exhibited enhanced antifungal activity against *Botrytis cinerea in vitro*, effectively suppressing gray mold in strawberries and maintaining fruit quality. In the $\gamma$-CD-MOF/eugenol composite developed by Cai's team [46], the eugenol loading rate was increased by 4.06 % compared to using $\gamma$-CD alone, along with significantly improved photostability and antioxidant properties. The composite demonstrated notable antifungal activity against *Fusarium graminearum* in both culture media and wheat grains, effectively extending grain storage time. In the field of drug delivery, CD-MOF-1 significantly enhances the delivery efficiency of volatile EO components. Zhou *et al*. [47] encapsulated D-limonene in $\gamma$-CD-MOF, increasing its pulmonary delivery bioavailability by 2.23-fold compared to oral administration. Zhu *et al*. [48] developed a eugenol nasal powder formulation (Eu@$\gamma$-CD-MOF) with a deposition distribution rate of 90.07 % ± 1.58 %, extending the nasal residence time of eugenol (Eu) from 5 min to 60 min. Through functional modification, CD-MOFs further expand their potential in intelligent controlled release and protection of EO components. Min *et al*. [49] incorporated $\gamma$-CD-MOF into chitosan-cellulose (CS-CEL) composite films by *in-situ* growth technology and encapsulated Car, constructing a humidity-responsive Car@$\gamma$-CD-MOFs/CS-CEL controlled-release system. This system releases Car upon humidity triggering, extending the shelf life of strawberries to 7 days. In summary, CD-MOFs demonstrate exceptional potential for EO delivery and functional enhancement, attributable to their three-dimensional porous structure, high specific surface area, and the synergistic effect of hydrophobicity and hydrophilicity on both internal and external surfaces.

### 2.5. Others

Beyond the major types of MOFs such as ZIFs, MILs, UiOs, IR-MOFs and CD-MOFs, other MOFs have also demonstrated application potential in the field of EO delivery. HKUST-1, a classic three-dimensional cage-like porous network structure of metal-organic frameworks developed by the Hong Kong University of Science and Technology, uses trimesic acid as the ligand and copper ions as the metal nodes, forming a three-dimensional channel system with a pore diameter of approximately 1 nm and a porosity of about 40 %, demonstrating advantages such as high specific surface area and unique pore characteristics [50]. Apart from HKUST-1, Porous coordination network materials (PCNs) have also attracted much attention in EO delivery due to their high specific surface area and excellent stability. Feng *et al*. [51] first proposed the synthesis of the PCN-222 series materials composed of zirconium clusters and metal porphyrins through a ligand elimination strategy. This series has an ultra-high specific surface area of 2600 $m^2/g$ and remains stable in extremely acidic environments. Both HKUST-1 and the PCN-222 series have the potential for encapsulating and delivering EOs. In addition, Bai *et al*. [52] prepared GR@MOF-545 by combining the photodynamic porphyrin MOF-545 with geraniol essential oil (GR). Under light exposure, it achieved an antibacterial rate of over 99 % against *E. coli* and *S. aureus*. Besides, compared with traditional MOFs, bio-metal-organic frameworks (Bio-MOFs) are MOFs constructed with natural biomolecules (such as amino acids, nucleotides, and polysaccharides) as core ligands or functional units [53]. Bio-MOFs endow materials with properties such as targeted

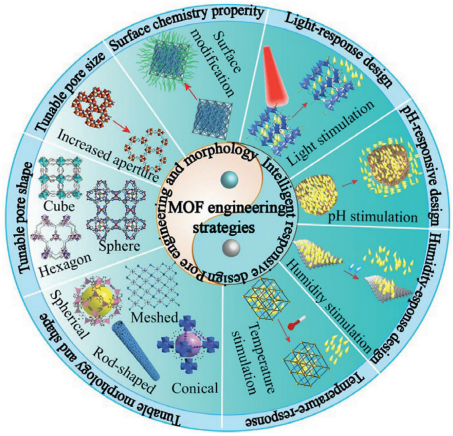



**Fig. 2.** The engineering strategies of MOFs including pore engineering (tunable pore size and pore shape), tunable morphology, surface chemical property, and intelligent response design.

delivery and biodegradability by integrating bioactive units. For instance, SION-19 was synthesized through the reaction among $Zn(NO_3)_2{\cdot}6H_2O$, 1,3,6,8-tetrakis(*p*-benzoic acid)pyrene ($H_4TBAPy$) and adenine. SION-19 can selectively capture thymine by hydrogen bonding and achieve adenine-thymine base pairing within its pore cavity, thereby mimicking the base recognition function of DNA [54]. Further, the delivery performance can be optimized by regulating the MOF structure through biological macromolecules, Chen *et al.* [55] developed a ZIF-8-based biocompatible strategy that utilized $\gamma$-poly-L-glutamic acid (PLGA) to regulate the transformation of nanostructures. Through a dual mechanism of promoting MOFs formation and inducing structural defects, it achieved the directional reconstruction from three-dimensional to two-dimensional mesoporous MOFs. This two-dimensional spindle-shaped mesoporous structure not only optimized the material exchange efficiency during the biotransformation process but also provided a stable protective environment for EO components.

## 3. Engineering strategies of MOFs for encapsulation, release and delivery of EOs

MOFs, owing to their unique physicochemical properties, have demonstrated substantial application potential in various fields, particularly in the encapsulation, release, and delivery of EOs. As natural products exhibiting diverse biological activities and aromatic characteristics, EOs possess broad application prospects in medicine, food, agriculture, and other domains. However, the poor stability and high volatility of EOs often limit their practical applications. MOF materials, characterized by their tunable structural features, provide effective solutions to these challenges. As illustrated in Fig. 2, this paper will focus on the key engineering strategies of MOFs, including pore engineering (adjustable pore size and shape), tunable morphology, surface chemical property, and intelligent response design, to elaborate on how these strategies enable efficient encapsulation, controlled release, and precise delivery of EOs. Table S2 (Supporting information) presents several application cases of MOFs in the delivery of EOs.

### 3.1. Pore engineering of MOFs for encapsulation and release of EOs

#### 3.1.1. The pore size of MOFs on release of EO

In the context of improving EO delivery strategies, the pore size of MOFs represents a critical structural parameter that governs both the loading capacity and release kinetics of the active components. Liu *et al.* [56] employed zirconium-based MOFs, specifically UiO-66, UiO-67, and UiO-68, which exhibit isomorphic characteristics, to systematically investigate how variations in pore size affect the loading and sustained release of terpene compounds (D-limonene, myrcene, $\alpha$-terpinene, and $\alpha$-pinene). The pore size parameters of the three MOFs increased in the order of 0.59, 0.71 and 0.94 nm. The study revealed that, except for $\alpha$-pinene, the loading capacities of the other three terpenes were significantly negatively correlated with the pore sizes of the MOFs. Specifically, the measured loading rates of myrcene in the three MOFs reached 90 %, 81 %, and 76 % of their respective theoretical saturation loading capacities. Release kinetics analysis demonstrated that only 16 % of the total loaded myrcene was released within a 24 h period in the UiO-67 system, which was substantially lower than the release levels observed for UiO-66 (49 %) and UiO-68 (62 %). Notably, D-limonene exhibited a cumulative release rate of 36.1 % in UiO-67, indicating superior sustained-release performance compared to UiO-66 (55.2 %) and UiO-68 (44.1 %).

#### 3.1.2. Tunable pore shapes of MOFs

MOFs exhibit a diverse range of pore structures and geometries, including triangles, hexagons, cubes, and spheres. The pore shape and architecture of MOFs play a crucial role in determining their capacity to load EOs. Liu *et al.* [56] emphasized that, in addition to pore size, the geometric shape of pores is also a critical factor influencing the loading capacity of MOFs for monoterpenoid components in EOs. Taking the rigid bicyclic structure of $\alpha$-pinene as an example, in the three MOFs UiO-66, UiO-67, and UiO-68, as the ratio of pore volume to pore diameter increases, the loading capacities of $\alpha$-pinene reach 16 %, 49 %, and 65 %, respectively. Notably, the triangular pore openings in UiO-66 significantly hinder the diffusion of $\alpha$-pinene molecules into the framework, resulting in the lowest loading capacity among the three materials. In addition, Zhang *et al.* [57] found that the differences in pore shapes of MOFs have a substantial influence on the diffusion behavior of active components in EOs. Specifically, UiO-66 crystals possess triangular channels, whereas ZIF-8 and ZIF-67 crystals both exhibit hexagonal channels. Using CT as the model compound, the diffusion behavior of CT in UiO-66, ZIF-8, and ZIF-67 was investigated and analyzed. The results revealed that the selectivity of Pt@ZIF-8 (>99 %) and Pt@ZIF-67 (>99 %) for CT was significantly higher than that of Pt@UiO-66 (6.69 %).

#### 3.1.3. The tunable morphology and shape of MOFs

In recent years, with the rapid development of MOFs, various forms of MOFs have been successfully developed, including rod-shaped, spherical, shuttle-shaped, spindle-shaped, one-dimensional straight chains, alternating or bundled chains, two-dimensional layered structures, central rectangular and snowflake-like, *etc.* [58,59] The shape and structure of MOFs affect the loading and release behavior of EOs components. For instance, ZIF-8 typically presents a polyhedral spherical or cubic form, while UiO-66 usually takes on an octahedral shape. Zuniega *et al.* [43] encapsulated the monoterpene components Thy and limonene from EOs at a 1:1 ratio into ZIF-8 and UiO-66-$(COOH)_2$ through a vapor diffusion method (16 h at 60 °C), followed by post-drying treatment at 30 °C. The results showed that the encapsulation efficiency of Thy in ZIF-8 and UiO-66-$(COOH)_2$ reached 36 % and 46 %, respectively. Moreover, at 25 °C, the Thy released from the MOF materials could significantly delay the growth of *Colletotrichum acutatum* for up to 6 days. Although the release concentration was lower than that of pure Thy, the volatile Thy released from UiO-66-$(COOH)_2$ still achieved a maximum inhibition rate of 40 % and continued to function after the peak growth period of the fungus, thereby significantly extending the action time of the EO components.

### 3.2. Surface chemistry of MOFs for encapsulation and prolonged release of EOs

Due to the wide variety of metal nodes and organic ligands, MOFs can almost achieve unlimited customized combinations, thereby demonstrating excellent tunability of chemical properties [60,61]. Surface engineering is one of the key strategies to achieve adjustable performance of MOFs, especially significant in the controlled release of volatile molecules. Chen *et al*. [62] successfully synthesized three different end-capped MIL-101 through amidation reactions and further regulated the release behavior of volatile molecules. The experimental results indicated that all three MOFs could effectively encapsulate volatile molecules and achieve sustained release effects ranging from several days to several months or even over a year. In addition to end-group modification, surface polarity regulation also has a significant impact on the adsorption and release behavior of EO components. Liu *et al*. [63] demonstrated that the adsorption capacity of polar ester fragrances on polar hydroxyl–functionalized MOFs was significantly higher than that on non-polar MOFs, while the adsorption behavior of non-polar terpene fragrances on the two types of MOFs showed no significant difference. The release curve analysis indicated that hydroxyl–functionalized MOFs could effectively prolong the release time of polar fragrances but have no significant effect on the release behavior of non-polar fragrances. Additionally, MOFs could be endowed with hydrophobic properties through post-synthetic modification approaches, such as introducing hydrophobic ligands or grafting hydrophobic functional groups onto the surface. Hydrophobic-modified MOFs exhibit significant hydrophobicity, effectively reducing the adsorption and penetration of water molecules, thereby enhancing the material's water resistance and moisture resistance and improving its stability in EO delivery [64,65]. Hydrophobic-modified MOFs have also been successfully applied in the design of multifunctional textiles, demonstrating excellent stability and practical application potential. The hydrophobic MOF@fabric prepared by Li *et al*. [66] demonstrated excellent superhydrophobic performance, with a water contact angle of $168.4^\circ \pm 1.6^\circ$, a rolling angle of $1.8^\circ \pm 0.2^\circ$, and an adhesion force as low as 16.17 μN. The material also exhibited excellent acid and base stability, and due to its superhydrophobic nature, its hydrolytic stability was significantly improved, remaining stable in water at 30 °C for 120 h without hydrolysis. In contrast, the non-hydrophobic MOF@fabric completely hydrolyzed its MOF crystal particles after being immersed in water at 30 °C for 6 h. Moreover, the prepared superhydrophobic MOF@fabric also demonstrated outstanding self-cleaning, anti-fouling, self-healing, UV resistance, and anti-icing properties, and could load natural antibacterial EOs, showing excellent antibacterial performance against *E. coli* and *S. aureus*.

### 3.3. Framework design of MOFs for stimulus-responsive release and delivery of EOs

With the ongoing integration of functional materials and intelligent release technologies, MOFs are increasingly recognized as ideal carriers for the intelligent controlled release of EOs. This is attributed to their highly tunable porous structures, versatile and customizable chemical properties, as well as their superior responsiveness to environmental stimuli. To address the challenges faced by EOs in practical applications, such as high volatility, poor stability, and uncontrollable release behavior, it is crucial to design MOF systems with intelligent response functions, thereby significantly enhancing the delivery efficiency and active functions of EOs. By modulating the internal structure, surface functional groups, and dynamic response units (*e.g.*, light-responsive, thermo-responsive, or pH-responsive groups), MOFs can be endowed with the ability to respond to single environmental factors (*e.g.*, temperature, humidity, light, pH) or multiple complex environmental factors (*e.g.*, the combined effect of pH value and enzymes, the coordinated change of pH value and temperature, the joint action of light and enzymes, magnetic fields). This design enables MOFs to achieve intelligent, stimuli-responsive release of EOs under various environmental conditions, thereby moving beyond the traditional "passive diffusion" mechanism and allowing for precise "on-demand release" control.

#### 3.3.1. pH-responsive design

The pH-responsive release strategy, as one of the intelligent delivery system strategies, provides an innovative solution to the bottlenecks of poor stability and insufficient environmental responsiveness of EO active components. ZIF-8, as a classic pH-responsive MOF, has shown promising application prospects in EO delivery. Ding *et al*. [26] developed a pH-responsive EO delivery system based on ZIF-8, which can specifically respond to pH changes in the microenvironment of diseases, thereby achieving controlled release of the EO CT for disease control. After 48 h of the experiment, the release amounts of CT in buffers with pH values of 3, 5, 7, and 9 were 80.97 %, 61.45 %, 36.66 %, and 27.32 %, respectively, further verifying the good responsiveness of this delivery system to pH stimuli. In different material systems, the design of pH response has different implementation methods and effects. Wang *et al*. [11] loaded the Eu onto the hierarchical porous structure of B-UiO-66 (benzoic acid-modified UiO-66) and constructed a synergistic antibacterial system, Eu@B-UiO-66/Zn, by complexing with zinc ions. This system achieved pH-responsive controlled release behavior of eugenol through the breaking of the coordination bond between eugenol and $Zn^{2+}$ ions as a "switch". Experimental results showed that within 96 h, the release rates of eugenol from Eu@B-UiO-66/Zn at pH 5.8 and pH 6.8 were 80 % and 58 %, respectively, while only 51 % was released at pH 8.0. Furthermore, after 24 h, the inhibition rates of Eu@B-UiO-66/Zn against *E. coli* and *S. aureus* reached 96.4 % and 99.7 %, respectively, which are markedly higher than those observed for free eugenol and the Eu@B-UiO-66 carrier alone.

#### 3.3.2. Humidity-response design

In addition to investigating the pH-responsive release properties of EOs loaded in MOFs, researchers have increasingly directed their attention toward studying humidity-responsive release behavior. Nong *et al*. [67] developed an edible $\beta$-CD-MOF/thymol@zein (BCCZ) composite film, which was prepared by combining Thy-loaded $\beta$-CD-MOF with zein. This film exhibited significant humidity-responsive drug release properties. The release behavior of Thy varied significantly under different humidity conditions: only 12.0 % was released within 7 days at 43 % relative humidity (RH), while the release amounts increased to 66.3 % and 96.3 % at 75 % and 100 % RH, respectively. The release rate increased with the rise in humidity. The humidity response mechanism of the film can be attributed to water molecules disrupting the K-O coordination bonds in the $\beta$-CD-MOF crystal structure, leading to structural decomposition and the release of encapsulated Thy. As a storage platform for Thy, the film enabled controlled release in high-humidity environments, effectively inhibiting common foodborne pathogens such as *S. aureus*, *E. coli*, and *Botrytis cinerea*. Humidity-responsive MOF materials with hierarchical structures enhance controlled release performance for targeted applications. Tian *et al*. [68] successfully constructed a composite hydrogel bead (TTO–HKUST-1@ALG) loaded with tea tree oil (TTO) based on the alginate/copper ion cross-linking strategy, combined with the *in-situ* growth and self-assembly technology of MOF. Due to the design of the hierarchical porous structure, the loading rate of TTO was significantly increased from 6.1 % to 21.6 %. This material

exhibited typical humidity-responsive sustained-release property. When the environmental humidity increased from 45 % to 95 %, the cumulative release rate of TTO linearly increased from 33.89 % to 70.98 %. This response mechanism originated from the high sensitivity of HKUST-1 to moisture, which contains a large number of unsaturated $Cu^{2+}$ coordination sites that are easily combined with water molecules. As alginate absorbs moisture and facilitates the coordination of water molecules with $Cu^{2+}$ ions, moisture disrupts the crystal structure of HKUST-1 through competitive adsorption, leading to the release of TTO.

*3.3.3. Temperature-response design*

Temperature-responsive release represents another critical form of intelligent response release in MOFs. Abdelhameed *et al.* [69] successfully prepared ZIF@MCC composite carriers by *in-situ* construction of zinc/cobalt-based ZIFs in microcrystalline cellulose (MCC) matrices. This material demonstrated thermos-responsive release characteristics for thyme and cumin EOs. Specifically, after 5 days of loading, the release rate of its active components was reduced by 23.6 % compared to pure MCC, with a clear positive correlation observed between temperature and release rate. Through the temperature regulation mechanism enabled by the mesoporous structure, the system could sustain EO release behavior over a 10-day cycle.

*3.3.4. Light-response design*

Light-responsive release is also a way to control the release of EOs from MOFs. It effectively addresses the common problems of drug burst release and concentration difficulty control in traditional continuous release systems through a time-space regulation mechanism. Meanwhile, due to its non-contact mode, it significantly enhances biological safety and application flexibility. Nong *et al.* [70] designed a composite system (FPZC: $Fe_3O_4$@polydopamine-COOH@ZIF-67/carvacrol) consisting of a $Fe_3O_4$ photothermal core, a polydopamine carboxylic acid shell layer, and a ZIF-67 coating structure, enabling near-infrared light-regulated controlled release of EOs. Experiments demonstrated that upon being triggered by an 808 nm laser for 60 s, 80 mg of the FPZC composite system could release 171 μg/L carvacrol vapor into the air, achieving complete inactivation of both *S. aureus* and *E. coli*. This technology demonstrated 100 % light-controlled sterilization efficiency and stability, effectively mitigating the biocompatibility risks associated with traditional contact-based antibacterial methods and showing promising application potential in food sterilization.

*3.3.5. Multi-stimuli responsive design*

In addition to the above-mentioned single-stimulus response, MOFs can also be used to construct delivery platforms with multi-stimulus response functions. Nong *et al.* [71] constructed a multifunctional nanozyme hybrid material based on MOF (FPMLC: $Fe_3O_4$@PVP@MIL-88B(Fe)-NH-lysozyme/carvacrol), which achieved highly efficient antibacterial activity through a multi-level synergistic mechanism. This material captured pathogenic bacteria by electrostatic adsorption and then formed a composite system through magnetic control assembly. The lysozyme component specifically hydrolyzed the peptidoglycan of the bacterial cell wall, while simultaneously releasing carvacrol under near-infrared excitation to disrupt the integrity of the cell membrane. Antibacterial results demonstrated that in a bacterial suspension of $1 \times 10^6$ CFU/mL, 100 μg/mL FPMLC could completely inactivate against *E. coli* and *S. aureus*. Owing to the structural flexibility and customizable properties of MOFs, researchers have developed intelligent delivery systems with multi-dimensional environmental sensing capabilities, thereby advancing the development of responsive materials toward precision and integration. Chen *et al.* [72] designed a MOF that responds to hypoxia/reactive oxygen species (ROS)/pH triple stimuli to achieve on-demand release of photosensitizers, thereby enhancing the efficacy of photodynamic therapy. This provided a theoretical basis for the triple-stimulus-responsive delivery of EOs and even multiple stimuli by MOFs.

## 4. Challenges of MOFs for delivery of EOs

### *4.1. Intelligent design challenge*

The design of MOFs with precisely tailored pore architectures for efficient encapsulation and controlled release of EOs represents a great challenge for their application in healthcare and food fields. Traditional MOFs design often optimizes pore parameters (*e.g.*, pore size and pore volume) based on limited experimental data (*e.g.*, the size of a single EO molecule). However, due to the complex composition of EOs (for instance, TTO contains over 30 active components), this approach may fail to fully account for the diverse molecular characteristics of all components [73]), their strong volatility, and susceptibility to oxidation and degradation, experience-driven pore regulation strategies face multiple challenges. On the one hand, MOFs need to simultaneously satisfy the differentiated loading requirements of multiple components: they must possess super-large channels to accommodate large terpene molecules while featuring micro-pores to confine small volatile molecules. On the other hand, the chemical environment on the pore surface (*e.g.*, the distribution of hydrophobicity/hydrogen bonding sites) must align with the polarity characteristics of EO components to prevent phase separation or loss of activity during the encapsulation process [74,75]. In recent years, computational and molecular dynamics simulation-guided strategies have emerged as a promising approach to address these challenges. By developing predictive models that correlate MOF topological networks with multi-component EO migration pathways, researchers can now inversely design MOF structures featuring gradient channels and heterogeneous surface sites. Such advanced architectures not only stabilize volatile monoterpenes through optimized host-guest interactions but also enable stimuli-responsive (*e.g.*, humidity/temperature-triggered) release by leveraging framework flexibility [76–79]. This intelligent design paradigm accelerates the development of MOF-based EOs delivery systems for applications ranging from medical dressings to smart packaging, while providing fundamental insights into long-term stabilization of volatile compounds and multimodal environmental responsiveness.

### *4.2. Challenges of large-scale productions*

Although MOF-based EO carriers exhibit promising properties at the molecular level, their industrial-scale implementation encounters three major challenges. First, scaling up the synthesis process while preserving high encapsulation efficiency remains a significant issue, as conventional solvothermal methods often result in structural defects during mass production [80,81]. To address this, Nankai University developed a high-pressure homogenization technique that enables molecular-level mixing, allowing to produce 0.96–580.48 tons/day of various porous materials with enhanced reproducibility and structural integrity [82]. Second, industrial loading processes face difficulties in controlling multi-component formulations. Traditional impregnation methods fail to achieve a gradient distribution of EO components, and open systems often lead to volatile losses [80]. Core-shell architectures, such as ZIF-8-on-ZIF-8, represent a notable advancement, enabling synchronous loading during shell formation and reducing release rates to 25 % of those observed with conventional carriers, while maintaining stability across a wide pH range (3–9) [83]. Finally,

cost-performance trade-offs pose a barrier to commercialization. MOFs that rely on precious metals are often economically impractical compared to traditional carriers. Recent alternatives include transition-metal-based ligands (*e.g.*, Fe/Co), which offer comparable performance at a lower cost [84], as well as cost-effective one-pot synthesis approaches using carboxylic acid ligands [85]. While these advancements in scalable production techniques (*e.g.*, high-pressure homogenization) and cost-reduction strategies (*e.g.*, alternative ligands) offer promising solutions, further optimization is essential to bridge the gap between laboratory-scale innovation and the industrial application of MOF-based EOs delivery systems.

### *4.3. Biological safety*

Biosafety assessment of MOF carriers represents a crucial challenge in their practical application. Current research indicates that cytotoxicity is primarily determined by three key factors: (1) Material composition, (2) particle characteristics, and (3) structural morphology. Some studies reveal considerable variations in the cytotoxic profiles of different MOFs. ZIF-8 exhibits size-dependent cytotoxicity, where 50 nm particles show a lower half-maximal inhibitory concentration ($IC_{50}$) value (15.6 μg/mL) compared to 200 nm particles (19.7 μg/mL) in HepG2 cells. This is attributed to the greater release of zinc ions and increased ROS generation from smaller particles [86]. In contrast, UiO-66 maintains over 85 % cell viability even at a high concentration of 200 μg/mL, owing to the stability of its zirconium-oxygen clusters [87]. Morphological studies show that spherical PCN-224 is more cytotoxic than rod-shaped PCN-222, with MOF-545 demonstrating the highest antibacterial activity among the tested structures [88]. Metal-ligand selection plays a critical role in determining the safety profile. While Cr(III)-MIL-100 exhibits minimal toxicity, its Fe(III)-based counterpart shows significant cytotoxic effects in Hep3B cells [89]. Moreover, the hydrophobicity of organic ligands in iron-based MOFs has been found to correlate linearly with $IC_{50}$ values [90]. Despite these findings, significant knowledge gaps persist concerning long-term *in vivo* effects, underlying molecular mechanisms, and potential bioaccumulation. Future research should prioritize investigations into degradation kinetics, excretion pathways, and the effects of chronic exposure to establish comprehensive safety guidelines for MOF-based delivery systems.

## 5. Conclusion and perspectives

Compared with previous reviews that focused on the application of MOF-delivered EOs in a single field, this paper innovatively integrates the functional requirements of EOs delivery with structural engineering strategies of MOFs. It systematically elaborates on MOF design approaches tailored to the molecular characteristics of EOs-such as pore size adjustment to match EO molecule dimensions and the incorporation of light-, temperature-, or pH-responsive functional sites to achieve spatiotemporal control over EOs release. This provides a comprehensive technical framework for the development of precise EO delivery systems. Furthermore, the paper identifies and critically discusses the great challenges hindering industrialization in this field, particularly the unique difficulties in intelligent design, bottlenecks in large-scale production, and key biosafety concerns specific to EOs delivery applications, thereby offering clear guidance for future research directions.

Future research should prioritize key areas such as material design optimization, innovation in release mechanisms, expansion of application scenarios, and comprehensive safety evaluation, to advance the development of MOF-based EO delivery systems. In material design, efforts should focus on developing low-cost, highly biocompatible MOFs and precisely regulating the pore environment through dynamic covalent chemistry strategies to accommodate the physicochemical properties of diverse EOs. Regarding release mechanisms, integrating multi-stimuli responsiveness-such as enzyme/pH/light co-triggering-with artificial intelligence prediction models can enable demand-driven release with precise spatiotemporal control. Additionally, the interdisciplinary synergies of MOF-EOs composite systems warrant further exploration, including the development of multifunctional food packaging films with both antibacterial and antioxidant properties or targeted nanoformulations for tumor-specific delivery of anti-cancer EOs, thereby expanding their application scope.

## Declaration of competing interest

The authors declare that they have no known competing financial interests or personal relationships that could have appeared to influence the work reported in this paper.

## CRediT authorship contribution statement

**Junfeng Huang:** Writing – original draft, Formal analysis. **Hongxin Chen:** Visualization. **Yan Liao:** Visualization. **Xiaowen Zhang:** Investigation. **Zengzhu Zhang:** Supervision, Formal analysis. **Xiaoyu Su:** Data curation. **Zihong Xie:** Investigation. **Biao Li:** Formal analysis. **Baode Shen:** Supervision. **Pengfei Yue:** Writing – review & editing, Supervision, Funding acquisition, Conceptualization.

## Acknowledgements

This work was partially supported by the National Natural Science Foundation of China (No. 82474087), the Natural Science Foundation of Jiangxi Province (No. 20242BAB26168), the Young Qihuang Scholar Program of Traditional Chinese Medicine of the State (No. 2022256), and Innovative Training Program for College Students of Jiangxi University of Chinese Medicine (Nos. S202510412137, 202510412040).

## Supplementary materials

Supplementary material associated with this article can be found, in the online version, at doi:10.1016/j.cclet.2025.112049.

## References

[1] K. Alirezalu, M. Pateiro, M. Yaghoubi, et al., Trends Food Sci. Technol. 100 (2020) 292–306.
[2] H.Y. Cui, C.H. Zhang, C.Z. Li, L. Lin, Ind. Crops Prod. 139 (2019) 111498.
[3] W. Thitinarongwate, W. Nimlamool, P. Khonsung, R. Mektrirat, P. Kunanusorn, Molecules 27 (2022) 4260.
[4] F. He, W. Wang, M.C. Wu, et al., Ind. Crops Prod. 153 (2020) 112552.
[5] K. Spyridopoulou, T. Aravidou, E. Lampri, et al., Antioxidants 10 (2021) 875.
[6] R. Kowalski, G. Kowalska, P. Mitura, et al., Molecules 29 (2024) 292.
[7] M. Corazza, G. Amendolagine, A. Borghi, G. Toni, M.M. Lauriola, Contact Dermatitis 81 (2019) 378–379.
[8] Q.Y. Huang, Y. Chen, M. Ye, et al., Mater. Today Chem. 40 (2024) 102235.
[9] X.Y. Liu, F. Xue, B. Adhikari, Sustain. Food Technol. 1 (2023) 426–436.
[10] B. Siu, A.R. Chowdhury, Z. Yan, S.M. Humphrey, T. Hutter, Coord. Chem. Rev. 485 (2023) 215119.
[11] J. Wang, L. Li, X.Y. Hu, L.L. Zhou, J. Hu, Dalton Trans. 53 (2024) 2826–2832.
[12] B. Zhao, J. Han, B. Liu, S.L. Zhang, B. Guan, Chem. Synth. 4 (2024) 41.
[13] X.Z. Yin, F.J. Ai, L.B. Han, Front. Chem. 10 (2022) 841316.
[14] X.C. Cai, X.G. Bao, Y.L. Wu, Pharmaceutics 14 (2022) 2641.
[15] I. Wagner, S. Spiegel, J. Brückel, et al., Macromol. Mater. Eng. 308 (2023) 2300048.
[16] J. Zhong, R.K. Kankala, S.B. Wang, A.Z. Chen, Polymers 11 (2019) 1627.
[17] B. Demirci, G. İşcan, A. Kaya, N. Saltan, Eur. J. Life Sci. 1 (2023) 112–117.
[18] L.H. Xie, M.M. Xu, X.M. Liu, M.J. Zhao, J.R. Li, Adv. Sci. 7 (2020) 1901758.
[19] R.R. Haikal, N. El Salakawy, A. Ibrahim, S.L. Ali, W. Mamdouh, Nanoscale Adv. 6 (2024) 4664–4671.
[20] P. Nezhad-Mokhtari, F. Kazeminava, B. Abdollahi, et al., Int. J. Biol. Macromol. 247 (2023) 125718.
[21] K. Zhang, D.L. Jin, X.M. Guo, et al., Ind. Crops Prod. 220 (2024) 119205.
[22] G.K. Angeli, M.I. Kotzabasaki, C. Maraveas, Appl. Sci. 15 (2025) 5479.

[23] M.A. Mohamud, A.B. Yurtcan, Int. J. Hydrogen Energy 46 (2021) 33782–33800.
[24] N.Y. Cheng, L. Ren, X. Xu, Y. Du, S.X. Dou, Adv. Energy Mater. 8 (2018) 1801257.
[25] K.S. Park, Z. Ni, A.P. Côté, et al., Proc. Natl. Acad. Sci. U. S. A. 103 (2006) 10186–10191.
[26] Y. Ding, J. Yuan, F.X. Mo, et al., J. Agric. Food Chem. 71 (2023) 18312–18322.
[27] P. Nezhad-Mokhtari, R. Rahbarghazi, H. Hamishehkar, P. Asadi, M. Milani, J. Polym. Environ. 32 (2024) 6211–6234.
[28] X.L. Huang, Y. Xing, H. Jiang, et al., J. Hazard. Mater. 472 (2024) 134502.
[29] T.T. Min, J. Yue, C.X. Cheng, et al., Chem. Eng. J. 496 (2024) 153686.
[30] X. Yang, M.E. Castell-Perez, R.G. Moreira, Z. Sevimli-Yurttas, J. Food Sci. 87 (2022) 4649–4664.
[31] G. Férey, C.M. Draznieks, C. Serre, et al., Science 309 (2005) 2040–2042.
[32] A. Schneemann, V. Bon, I. Schwedler, et al., Chem. Soc. Rev. 43 (2014) 6062–6096.
[33] A.V. Neimark, F.X. Coudert, C. Triguero, et al., Langmuir 27 (2011) 4734–4741.
[34] A.F. Sapnik, D.N. Johnstone, S.M. Collins, et al., Dalton Trans. 50 (2021) 5011–5022.
[35] K. Caamaño, R. Heras-Mozos, J. Calbo, et al., ACS Appl. Mater. Interfaces 14 (2022) 10758–10768.
[36] A.M. Pak, E.A. Maiorova, E.D. Siaglova, et al., Nanomaterials 13 (2023) 1714.
[37] J.H. Cavka, S. Jakobsen, U. Olsbye, et al., J. Am. Chem. Soc. 130 (2008) 13850–13851.
[38] M. Kandiah, M.H. Nilsen, S. Usseglio, et al., Chem. Mater. 22 (2010) 6632–6640.
[39] H. Wu, Y.S. Chua, V. Krungleviciute, et al., J. Am. Chem. Soc. 135 (2013) 10525–10532.
[40] Z. Wang, S.G. Hu, J. Yang, et al., Adv. Funct. Mater. 28 (2018) 1707356.
[41] R. Abazari, S. Sanati, M.A. Bajaber, et al., Small 20 (2023) e2306353.
[42] M.H. Zheng, Y.L. Huang, W.W. Hu, et al., ACS Appl. Mater. Interfaces 16 (2024) 36017–36029.
[43] J. Zuniega, J. Grabulos, M. Lebrun, et al., Int. J. Food Sci. Technol. 59 (2023) 730–742.
[44] Y.Z. He, W. Zhang, T. Guo, et al., Acta Pharm. Sin. B 9 (2019) 97–106.
[45] L.L. Yu, X.X. Wang, Y.Y. Wei, et al., Food Control 155 (2024) 110053.
[46] L.Z. Cai, L. Li, D. Li, et al., Ind. Crops Prod. 221 (2024) 119314.
[47] Y. Zhou, M.J. Zhang, C.F. Wang, et al., Int. J. Pharm. 606 (2021) 120825.
[48] H.J. Zhu, Y.T. Lv, F.Y. Xin, et al., AAPS PharmSciTech 25 (2024) 117.
[49] T.T. Min, Y.J. Lei, C.X. Cheng, et al., Food Hydrocolloids 150 (2024) 109633.
[50] M. Hartmann, S. Kunz, D. Himsl, O. Tangermann, Langmuir 24 (2008) 8634–8642.
[51] D. Feng, W.C. Chung, Z. Wei, et al., J. Am. Chem. Soc. 135 (2013) 17105–17110.
[52] H.R. Bai, L.Y. Yang, L. Wu, D.X. Xiao, A. Dong, Chem. Eng. J. 498 (2024) 155503.
[53] H. Cai, Y.L. Huang, D. Li, Coord. Chem. Rev. 378 (2019) 207–221.
[54] S.L. Anderson, P.G. Boyd, A. Gładysiak, et al., Nat. Commun. 10 (2019) 1612.
[55] G. Chen, S. Huang, X. Kou, F. Zhu, G. Ouyang, Angew. Chem. Int. Ed. 59 (2020) 13947–13954.
[56] Y.H. Liu, Y.J. Zhao, Z.X. Zhou, Y.Q. Shen, L.M. Jiang, Colloids Surf. A 674 (2023) 131907.
[57] W.L. Zhang, W.X. Shi, W.L. Ji, et al., ACS Catal. 10 (2020) 5805–5813.
[58] Y.S. Lin, K.S. Lin, Microporous Mesoporous Mater. 328 (2021) 111456.
[59] D.P. Lyu, W. Xu, J.E.L. Payong, T. Zhang, Y. Wang, Nat. Commun. 13 (2022) 3980.
[60] S.H. Tu, A.R. Liu, H.X. Zhang, et al., Chin. Chem. Lett. 35 (2024) 109761.
[61] H. Wang, M.Q. Pan, Y.F. Wang, et al., Chin. Chem. Lett. 35 (2024) 109581.
[62] H.W. Chen, H.Q. Chen, B. Zhang, et al., Chin. Chem. Lett. 32 (2021) 1988–1992.
[63] Y.H. Liu, Y.X. Wang, J.X. Huang, et al., AlChE J. 65 (2018) 491–499.
[64] K.L. Miller, R. Lin, J. Hou, et al., Mater. Adv. 5 (2024) 1868–1874.
[65] D.A. Evangelou, A.D. Pournara, V.I. Karagianni, et al., ACS Appl. Mater. Interfaces 16 (2024) 12672–12685.
[66] W.L. Li, Y.X. Zhang, Z. Yu, et al., ACS Nano 16 (2022) 14779–14791.
[67] W.Q. Nong, H.L. Luo, G. Wang, et al., Carbohydr. Polym. 351 (2025) 123133.
[68] Y.Q. Tian, L. Zhou, J.P. Liu, et al., Food Chem. 451 (2024) 139440.
[69] R.M. Abdelhameed, E. Alzahrani, A.A. Shaltout, H.E. Emam, J. Ind. Eng. Chem. 94 (2021) 134–144.
[70] W.Q. Nong, W.L. Guan, Y. Yin, et al., Chem. Eng. J. 420 (2021) 129874.
[71] W.Q. Nong, Y.L. Chen, D.Y. Lv, et al., Chem. Eng. J. 431 (2022) 134003.
[72] W.Y. Chen, H.X. He, P.F. Jiao, et al., Adv. Healthc. Mater. 12 (2023) e2301785.
[73] P. Malik, P. Upadhyay, Orient. J. Chem. 38 (2022) 1266–1275.
[74] Y. Yao, X.Y. Zhao, G.G. Chang, X.Y. Yang, B. Chen, Small Struct. 4 (2022) 2370001.
[75] T.H. Lan, L.B. Li, Y. Chen, et al., Mater. Chem. Front. 4 (2020) 1954–1984.
[76] R.B. Lin, Z.J. Zhang, B.L. Chen, Acc. Chem. Res. 54 (2021) 3362–3376.
[77] A. Sturluson, M.T. Huynh, A.R. Kaija, et al., Mol. Simul. 45 (2019) 1082–1121.
[78] D.M. Feng, C.F. Wang, Y. Liu, et al., J. Oleo Sci. 72 (2023) 957–968.
[79] P.Z. Moghadam, Y.G. Chung, R.Q. Snurr, Nat. Energy 9 (2024) 121–133.
[80] U.J. Ryu, S. Jee, P.C. Rao, et al., Coord. Chem. Rev. 426 (2021) 213544.
[81] I. Thomas-Hillman, A. Laybourn, C. Dodds, S.W. Kingman, J. Mater. Chem. A 6 (2018) 11564–11581.
[82] X.L. Liu, A. Wang, C.P. Wang, et al., Nat. Commun. 14 (2023) 7022.
[83] T.C. Huang, X.J. Cui, X.Y. Zhou, et al., Materials 17 (2024) 1310.
[84] Y.C. Yang, Y.W. Yang, Y.Y. Liu, S.L. Zhao, Z.Y. Tang, Small Sci. 1 (2021) 2100015.
[85] X.J. Kong, T. He, Y.Z. Zhang, et al., Chem. Sci. 10 (2019) 3949–3955.
[86] P.Y. Chen, M. He, B.B. Chen, B. Hu, Ecotoxicol. Environ. Saf. 205 (2020) 111110.
[87] M. Ding, B. Moreira-Álvarez, F.C. Celis, et al., RSC Adv. 14 (2024) 1676–1685.
[88] Y.Y. Liu, L.J. Chen, X. Zhao, X.P. Yan, Chem. Eur. J. 27 (2021) 10151–10159.
[89] R. Grall, T. Hidalgo, J. Delic, et al., J. Mater. Chem. B 3 (2015) 8279–8292.
[90] C. Tamames-Tabar, D. Cunha, E. Imbuluzqueta, et al., J. Mater. Chem. B 2 (2014) 262–271.